

Aromaticity in Stable Tiara Nickel Thiolates: Computational and Structural Analysis

Ayan Datta,[†] Neena S. John,[‡] G. U. Kulkarni,[‡] and Swapan K. Pati^{*,†}*Theoretical Sciences Unit, Chemistry and Physics of Materials Unit, and DST Unit on Nanoscience, Jawaharlal Nehru Center for Advanced Scientific Research, Jakkur P. O, Bangalore-560064, India**Received: September 20, 2005; In Final Form: November 6, 2005*

Quantum chemical calculations as well as crystallographic analyses show that the Ni_n rings in the tiara Ni thiolates, $[NiS_2]_n$ and $[Ni(SR)_2]_n$ ($n = 3-6$), have highly symmetric polygonal structures. We find that such structural features primarily arise from the effective delocalization of the d-orbital electrons across the Ni_n rings leading to bond length equalization and thereby aromaticity. We introduce the d-orbital aromaticity for the first time to explain the experimentally observed polygonal structures of these cyclic metal rings bridged by thiol linkages.

Aromaticity is a fundamental concept in chemistry, and the meticulous success of simple yet effective Huckel rules in explaining a large body of experimental results in organic molecules is really commendable.^{1,2} The recent progress in the area of experimental characterization of small inorganic molecules in the form of cyclic Al and Sn atomic clusters has extended the concept of aromaticity to the realms of metal systems.^{3,4} Recently d-orbital aromaticity in coinage metals has been reported.⁵ In the same context, metal thiolates exhibiting symmetric cyclic structures are of great interest, not just because of their unusual stability, but also because of their biological importance as active sites in enzymes.⁶⁻⁸ However, there exists no rationalization for the unusual stability of the metal rings in these thiolates. In the only theoretical report available on toroidal Ni thiolates, metal-metal interactions have been claimed to be quite weak.⁸ In this communication, based on computational and structural analysis, we show that the Ni_n rings of Ni thiolates have a tendency toward strong d-electron delocalization that results in aromaticity in these symmetric polygonal structures. For the first time, we introduce the concept of aromaticity to critically understand the structural features associated with stability in these d^8 systems. Ni thiolates are used as templates for nanostructures,⁹ and the introduction of a central concept like aromaticity can aid in better understanding and prediction of the properties of such materials.

In this study, we consider cyclic $[NiS_2]_n$ and $[Ni(SR)_2]_n$ ($n = 3, 4, 5$, and 6) systems with $R = CH_3, C_2H_5, C_3H_7, C_4H_9$, and C_5H_{11} . The global optimized geometries for these molecules were derived at the B3LYP/LANL2MB level available with the *Gaussian 03* set of programs.¹⁰ In Figure 1, we show the optimized structures of the Ni thiolates for an intermediate alkyl chain length, $R = C_2H_5$. The corresponding structural parameters are given in Table 1. The cyclic architectures have a planar Ni_n backbone, which is perfectly polygonal with the $\angle Ni-Ni-Ni$ very close to the exact $(n-2) \times 180/n$ value (see Table 1). In both the computed and the experimental structures, the Ni-Ni distance increases with an increase in nuclearity of the tiara

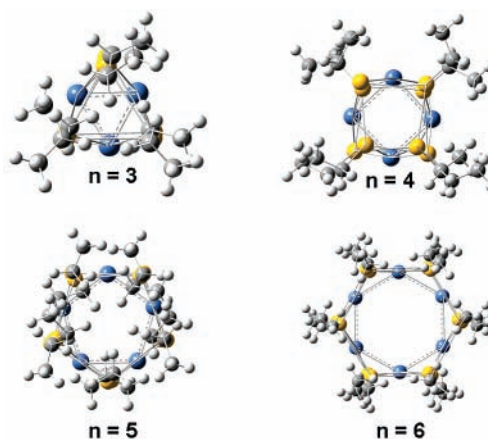


Figure 1. Ground-state geometries for cyclic $[Ni(SR)_2]_n$ ($R = C_2H_5$) for $n = 3, n = 4, n = 5$, and $n = 6$. Note that Ni atoms share the edges of a regular polygon.

TABLE 1: Variations of the Ni-Ni Distances (in Å) and Polygonal Angle and trans S-Ni-S Angle (both in deg) for the Optimized and Experimental Molecules of $[Ni(SC_2H_5)_2]_n^a$

n	$d(Ni-Ni)$ computed (exptl)	$\angle Ni-Ni-Ni$ computed (exptl)	$\angle_{trans} S-Ni-S$ computed (exptl)
3	2.61 (2.64)	59.9 (59.72)	160.7 (150.04)
4	3.02 (2.66)	90.17 (89.25)	167.3 (168.89)
5	3.14 (2.82)	107.96 (107.97)	178.48 (171.15)
6	3.35 (2.92)	120.02 (119.99)	179.6 (177.50)

^a See ref 11 for CSD codes for the experimental molecules. Only the cyclic portion of the molecule is considered.

complex. The differences observed in the Ni-Ni distances between the computed and the experimental structures are mainly due to the ligands that are attached to sulfur in the latter case, in addition to the kinetic factors that are involved in the stabilization of the crystal structures. The trimeric ($n = 3$) structure represents maximum pyramidal distortion with small Ni-Ni distance that incorporates ring strain analogous to cyclopropane. On the other hand, the Ni_6 ring is hexagonal, very similar to benzene. These systems thus themselves offer for comparison with their organic counterparts.

* pati@jncasr.ac.in.

[†] Theoretical Sciences Unit and DST Unit on Nanoscience.

[‡] Chemistry and Physics of Materials Unit and DST Unit on Nanoscience.

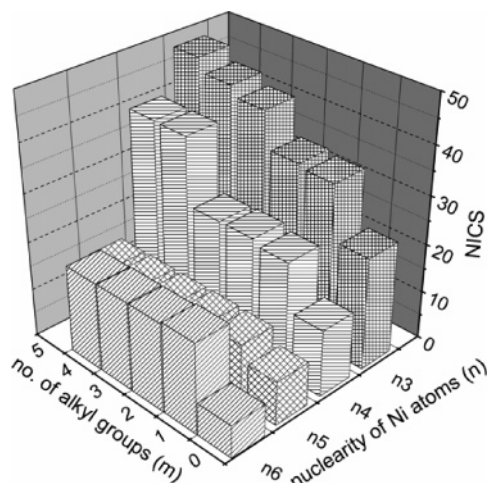


Figure 2. GIAO/NICS values (in ppm) for the tiara complexes with increasing numbers of methyl groups (m) and increasing nuclearity (n). Note that all NICS values are positive.

The $\angle_{\text{trans S-Ni-S}}$ measures the extent of pyramidalization, and a value of 180° represents perfect planarity of the Ni atom with the neighboring S_4 ring. Thus, the value, $(180 - \text{trans S-Ni-S})^\circ$ quantifies the pyramidalization. As seen from Table 1, the pyramidalization angle decreases with increase in n .

Furthermore, with increase in ring size, n , the tendency for distortion in the S_4 ring increases, and as a result, the square-like S_4 ring in the trimer gets distorted into a rectangular geometry in the case of a hexamer with bond length alternation (BLA) of 0.73 \AA . In fact, such a distortion reduces the pyramidalization of the Ni atom and brings the Ni atoms in-plane with the S_4 ring. Similar trends have been observed with a variation of alkyl chain lengths.

To quantify aromaticity in these systems, we have calculated the magnetic properties, viz., nucleus-independent chemical shifts (NICS) at the center of the Ni_n rings at the GIAO/RB3LYP LANL2MB level (see Figure 2).¹²

As seen from the Figure 2, the magnitude for NICS in all these systems is however positive. For a given nuclearity (n), NICS increases with an increase in the number of alkyl groups (m). For example, for $n = 3$, the magnitude of NICS increases from 22 to 48 ppm for $R = 0$ to $R = C_5H_{11}$. This is revealed in the Mulliken charges as well. The charge on the S atom increases from $-0.28 e$ to $-0.45 e$ ($R = 0$ to C_5H_{11}), following an increase in the +I (inductive) effects of the alkyl groups resulting in charge localization on the bridged S atoms. This in turn reduces charge transfer between the Ni atoms, thereby the diamagnetic current (aromaticity). Also, very interestingly, NICS tends to decrease with the nuclearity (n), suggesting more facile delocalization for the larger tiara complexes compared to the smaller nuclearity systems. This is consistent with the smaller pyramidalization angles associated with the Ni atoms in larger-nuclearity rings.

Note that, for simple organic molecules, a positive NICS value (paramagnetic ring current) suggests antiaromaticity, and they are expected to be distorted (nonzero BLA). However, the structures for all the Ni_n rings are perfectly planar polygonal, invariably suggesting aromatic characteristics. To have a better understanding of aromaticity/antiaromaticity in these systems, we perform a detailed analysis of the contributions of the 3d orbitals and the core orbitals (3s and 3p) of the Ni atoms and the 3p and 3s orbitals of the S atoms to all the molecular orbitals. The squares of these amplitudes summed up for all the Ni and S atoms separately for each molecular orbital are shown in Figure 3, for the hexameric Ni_6 ring with $R = C_2H_5$.

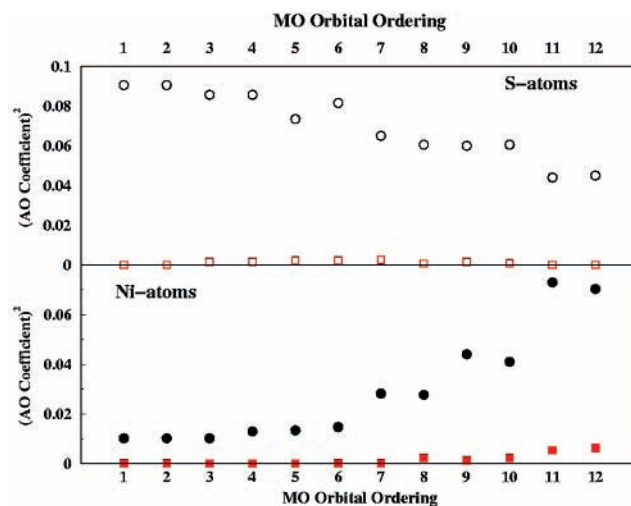


Figure 3. Upper panel: Contributions from the 3p orbitals (open circles) and the 3s orbitals (open red squares) from the sulfur atoms to MOs. Lower panel: Contributions from the 3d orbitals (filled circles) and the core 3s and 3p orbitals (closed red squares) from the nickel atoms to MOs. Note that the MOs are shown from HOMO to HOMO - 11, viz., 1st MO = HOMO and 12th MO = HOMO - 11.

As can be seen, the frontier orbitals (from HOMO to HOMO - 5) have very little contributions from the 3d orbitals of the Ni atoms (~ 0.01), and the major contributions arise from the 3p orbitals of the S atoms. The contributions from the core orbitals for both Ni and S are very small for all the MOs. Thus, these frontier orbitals do not possess extended conjugation across the Ni and S atoms and thus essentially show antiaromaticity. However, as one considers the lower-energy orbitals (HOMO - 6 and below), the contributions from the 3d orbitals of the Ni atoms start to increase by more than twofold, and in particular, the HOMO - 10 and HOMO - 11 have very large contributions from the 3d orbitals of Ni. Also, very interestingly for these orbitals, the contributions from the 3p orbitals of sulfur atoms are also similar (~ 0.06). Therefore, it leads to extended delocalization across the Ni_n ring with almost equal contributions from the Ni atoms and the S atoms.

The origin for the antiaromatic nature of the frontier orbitals is traced back to the symmetry of the d orbitals of the Ni atoms and the p orbitals of the S atoms involved in MO formation. For example, in the frontier MOs, the only contributing d orbitals are the d_{xz} and d_{yz} orbitals, while the major contributions from the S atoms arise from the $3p_y$ and $3p_z$ orbitals. This results in poor overlap between the Ni and S atoms of the ring. However, for the low-energy MOs, the major contributions from the 3d orbitals are from the d_{z^2} , $d_{x^2-y^2}$, and d_{xy} orbitals. Note that these orbitals possess the correct symmetry to undergo effective overlap with the S orbitals because of the square planer geometry of Ni. Thus, the low-energy orbitals are highly delocalized.

Such multiple aromaticity features (antiaromatic frontier orbitals and aromatic low-energy orbitals) are also evident from the plots of the highly delocalized orbitals. We have plotted the lowest-energy orbitals, which fully share conjugations across the Ni_n ring for four n values in Figure 4. This is in sharp contrast to the p_π conjugated aromatic systems like C_6H_6 , where the frontier orbitals are highly delocalized.

Thus, the highly symmetric structures in Ni_n arise from the greatly favorable delocalization of the d electrons in low-energy orbitals that lead to equalization of all the Ni-Ni bonds in the polygon. Here, we would like to point out that such an analysis is well-established for even simple molecules such as C_6H_6 , where the low-energy σ orbitals force a highly symmetric

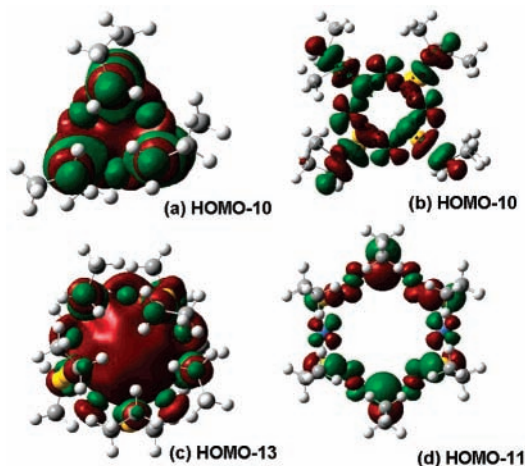


Figure 4. Highly delocalized MOs for (a) trimer, (b) tetramer, (c) pentamer, and (d) hexamer.

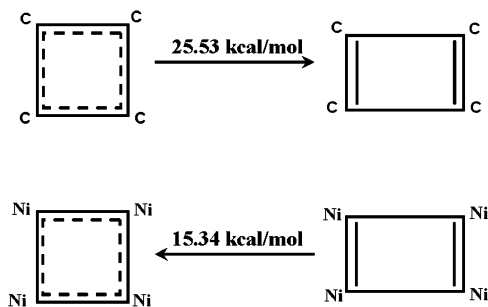


Figure 5. Representation of favorable JT distortion in C_4H_4 (upper panel) and favorable D_{4h} structure of Ni_4 (lower panel) compared to the distorted D_{2h} geometry. Note that the H-atoms in C_4H_4 and S-atoms/ethyl groups in $[Ni(SR)_2]_4$ are not shown for clarity.

structure, while the π electrons of the frontier orbitals have an overwhelming tendency for a distorted D_{3h} structure. The overall structure is of course governed by the more predominating σ equalization over the π distortion.¹³ It is interesting to observe very similar features in these transition-metal complexes as well. The aromatic nature of these Ni thiolates is also evident from the fact that these structures do not exhibit the conventional antiaromatic Jahn–Teller (JT) distorted geometry like that in C_4H_4 . This is schematically shown in Figure 5, by comparing the distortion energies for C_4H_4 and its analogue, tetranuclear Ni thiolate. JT distortion in the D_{4h} square structure of C_4H_4 leads to a stabilization of 25.5 kcal/mol and thereby stabilizes the D_{2h} structure with BLA of 0.24 Å. However, the case for the Ni_4 ring in $[Ni(SR)_2]_4$ ($R = C_2H_5$) is exactly opposite. In fact, JT distortion destabilizes the Ni system by 15.3 kcal/mol (for the same BLA as in C_4H_4). Thereby, for Ni thiolates, the highly symmetric D_{4h} square geometry corresponds to the ground state.

The binding energies (defined as $E_{\text{tiara}} - nE_{\text{single}}$) also increase with an increase of the ring sizes, suggesting larger aromaticity for the larger Ni_n rings. For example, for $R = C_2H_5$, the binding energies are -266.43 kcal/mol ($n = 3$), -417.08 kcal/mol ($n = 4$), -431.05 kcal/mol ($n = 5$), and -447.86 kcal/mol ($n = 6$). Thus, these Ni thiolates are quite stable and are effectively aromatic. Interestingly, in the larger clusters ($n = 4$ – 6), the stability increases linearly with cluster size, suggesting the absence of odd–even effects in these systems as opposed to alkane chains¹⁴ or clusters of atoms with only s or p orbitals.¹⁵

To the best of our knowledge, this is the first case of detailed analysis of the structures in Ni_n rings based on aromaticity. In fact, the JT distortion that arises from the electron–phonon

interactions (V_{en}) is fully quenched in these thiolates, thereby giving rise to a rectangular planar environment of the NiS_4 units, more so for the larger chain lengths. These structures are stabilized by the strongly delocalized low-energy d orbitals. The S atoms above and below the Ni_n planes fix the metal ions in a rectangular planar geometry, thereby preventing distortions in the Ni_n rings. Our theoretical calculations provide the microscopic understanding of the experimental observation of highly symmetric tiara Ni thiolates with large but finite nuclearity.

Acknowledgment. N.S.J. acknowledges CSIR for financial assistance. G.U.K. and S.K.P. thank CSIR, DRDO, and DST, Govt. of India for research grants. The authors thank Prof. C. N. R. Rao for encouragement.

References and Notes

- (1) (a) Minkin, V. I.; Glukhovtsev, M. N.; Simkin, B. Ya. *Aromaticity and Antiaromaticity*; Wiley: New York, 1994. (b) Burley, G. A. *Angew. Chem., Int. Ed.* **2005**, *44*, 3176.
- (2) (a) Gomas, J. A. N. F.; Mallion, R. B. *Chem. Rev.* **2001**, *101*, 1349. (b) Boldyrev, A. I.; Wang, L.-S. *Chem. Rev.* **2005**, *105*, 3716.
- (3) (a) Li, X.; Kuznetsov, A.; Zhang, H.-F.; Boldyrev, A. I.; Wang, L. *Science* **2001**, *291*, 859. (b) Li, X.; Zhang, H.-F.; Wang, L.-S.; Kuznetsov, A. E.; Cannon, N. A.; Boldyrev, A. I. *Angew. Chem., Int. Ed.* **2001**, *40*, 1867. (c) Kuznetsov, A.; Boldyrev, A. I.; Li, X.; Wang, L.-S. *J. Am. Chem. Soc.* **2001**, *123*, 8825. (d) Datta, A.; Pati, S. K. *J. Chem. Theory Comput.* **2005**, *1*, 824. (e) Datta, A.; Pati, S. K. *Chem. Commun.* **2005**, 5032.
- (4) (a) Kuznetsov, A.; Boldyrev, A. I.; Li, X.; Wang, L.-S. *J. Am. Chem. Soc.* **2001**, *123*, 8825. (b) Kuznetsov, A.; Birch, K.; Boldyrev, A. I.; Li, X.; Zhai, H.; Wang, L. *Science* **2003**, *300*, 622. (c) Datta, A.; Pati, S. K. *J. Am. Chem. Soc.* **2005**, *127*, 3496. (d) Chen, Z.; Corminboeuf, C.; Heine, T.; Bohmann, J.; Schleyer, P. v. R. *J. Am. Chem. Soc.* **2003**, *125*, 13930. (e) Xu, Q.; Jiang, L.; Tsumori, N. *Angew. Chem., Int. Ed.* **2005**, *44*, 4338.
- (5) (a) Wannere, C. S.; Corminboeuf, C.; Wang, Z.-X.; Wodrich, M. D.; King, R. B.; Schleyer, P. v. R. *J. Am. Chem. Soc.* **2005**, *127*, 5701. (b) Tshipis, A. C.; Tshipis, C. A. *J. Am. Chem. Soc.* **2003**, *125*, 1136. (c) Li, S.-D.; Ren, G.-M.; Miao, C.-Q.; Jin, Z. H. *Angew. Chem., Int. Ed.* **2004**, *43*, 1371.
- (6) (a) Dance, I. G. *Polyhedron* **1986**, *5*, 1037. (b) Mahmoukhani, A. H.; Langer, V. *Polyhedron* **1999**, *18*, 3407. (c) Watson, A. D.; Pulla Rao, C.; Dorfman, J. R.; Holm, R. H. *Inorg. Chem.* **1985**, *24*, 2820. (d) Li, Z.; Ohki, Y.; Tatsumi, K. *J. Am. Chem. Soc.* **2005**, *127*, 8950.
- (7) Nobusada, K.; Yamaki, T. *J. Phys. Chem. A* **2004**, *108*, 1813.
- (8) Alemany, P.; Hoffmann, R. *J. Am. Chem. Soc.* **1993**, *115*, 8290.
- (9) (a) Ghezlbash, A.; Sigman, M. B., Jr.; Korgel, B. A. *Nano Lett.* **2004**, *4*, 537. (b) Larsen, T. H.; Sigman, M. B.; Ghezlbash, A.; Doty, R. C.; Korgel, B. A. *J. Am. Chem. Soc.* **2003**, *125*, 5638. (c) John, N. S.; Thomas, P. J.; Kulkarni, G. U. *J. Phys. Chem. B* **2003**, *107*, 11376.
- (10) Frisch, M. J.; Trucks, G. W.; Schlegel, H. B.; Scuseria, G. E.; Robb, M. A.; Cheeseman, J. R.; Montgomery, J. A., Jr.; Vreven, T.; Kudin, K. N.; Burant, J. C.; Millam, J. M.; Iyengar, S. S.; Tomasi, J.; Barone, V.; Mennucci, B.; Cossi, M.; Scalmani, G.; Rega, N.; Petersson, G. A.; Nakatsuji, H.; Hada, M.; Ehara, M.; Toyota, K.; Fukuda, R.; Hasegawa, J.; Ishida, M.; Nakajima, T.; Honda, Y.; Kitao, O.; Nakai, H.; Klene, M.; Li, X.; Knox, J. E.; Hratchian, H. P.; Cross, J. B.; Bakken, V.; Adamo, C.; Jaramillo, J.; Gomperts, R.; Stratmann, R. E.; Yazyev, O.; Austin, A. J.; Cammi, R.; Pomelli, C.; Ochterski, J. W.; Ayala, P. Y.; Morokuma, K.; Voth, G. A.; Salvador, P.; Dannenberg, J. J.; Zakrzewski, V. G.; Dapprich, S.; Daniels, A. D.; Strain, M. C.; Farkas, O.; Malick, D. K.; Rabuck, A. D.; Raghavachari, K.; Foresman, J. B.; Ortiz, J. V.; Cui, Q.; Baboul, A. G.; Clifford, S.; Cioslowski, J.; Stefanov, B. B.; Liu, G.; Liashenko, A.; Piskorz, P.; Komaromi, I.; Martin, R. L.; Fox, D. J.; Keith, T.; Al-Laham, M. A.; Peng, C. Y.; Nanayakkara, A.; Challacombe, M.; Gill, P. M. W.; Johnson, B.; Chen, W.; Wong, M. W.; Gonzalez, C.; Pople, J. A. *Gaussian 03*, revision B.05; Gaussian, Inc.: Pittsburgh, PA, 2003.
- (11) CONQUEST, version 1.7; Cambridge Crystallographic Database; CCSD, 2004. CSD Codes: trimer, PCNTNI; tetramer, CELXAS.; pentamer, FOTVEP.; hexamer: JOXMOY.
- (12) Schleyer, P. v. R.; Maerker, C.; Dransfeld, A.; Jiao, H.; Eikema-Hommas, N. J. R. V. *J. Am. Chem. Soc.* **1996**, *118*, 6317.
- (13) (a) Shaik, S. S.; Hiberty, P. C. *J. Am. Chem. Soc.* **1985**, *107*, 3089. (b) Shaik, S. S.; Hiberty, P. C.; Lefour, J.-M.; Ohanessian, G. *J. Am. Chem. Soc.* **1987**, *109*, 363.
- (14) (a) Asha, S. K.; Kavita, K.; Das, P. K.; Ramakrishnan, S. *Chem. Mater.* **1999**, *11*, 3352. (b) Datta, A.; Pati, S. K.; Davis, D.; Sreekumar, K. *J. Phys. Chem. A* **2005**, *109*, 4112.
- (15) (a) Chandrakumar, K. R. S.; Ghanty, T. K.; Ghosh, S. K. *J. Phys. Chem. A* **2004**, *108*, 6661. (b) Datta, A.; Pati, S. K. *Comput. Lett.* In press.